

Supporting information

Stainless steel-derived nano-porous oxide: A cost-efficient, stable, and corrosion-resistant hydrogen evolution catalyst.

Ranjith Bose^{1,2,*}, Surya Prakash Gajagouni³, Imad Barsoum³, Sung Oh Cho⁴, and Akram Alfantazi^{1,2,*}

¹*Department of Chemical and Petroleum Engineering, Khalifa University, Abu Dhabi 127788, United Arab Emirates.*

²*Emirates Nuclear Technology Center (ENTC), Khalifa University, Abu Dhabi 127788, United Arab Emirates.*

³*Department of Mechanical and Nuclear Engineering, Khalifa University, Abu Dhabi 127788, United Arab Emirates.*

⁴*Department of Nuclear and Quantum Engineering, Korea Advanced Institute of Science and Technology (KAIST), Daejeon 34141, South Korea.*

Corresponding author: Dr. Ranjith Bose and Prof. Akram Alfantazi
E-mail: ranjith.bose@ku.ac.ae and akram.alfantazi@ku.ac.ae

TABLE OF CONTENT

Materials Characterization	
Electrochemical measurements	
Figure S1	Digital images of anodization experiments
Figure S2	Digital images of prepared samples
Figure S3	SEM and Cross-section images of bare SS, and anodized SS samples
Figure S4	EDX spectrum of bare SS
Figure S5	Low and high magnification SEM and Cross-sectional images of anodized SS (SS-65 V and SS-85 V) samples
Figure S6	Low and high-magnification SEM images of anodized SS- 90 V sample
Figure S7	Schematic illustration of anodized stainless steel
Figure S8	XRD patterns of bare SS and anodized SS samples
Figure S9	XPS survey spectrum of SS-75 V sample
Figure S10	Long-term chronoamperometric (CA) stability measurement at -100 mA cm ⁻² for the SS-75 V electrode.
Figure S11	CV curves for anodized SS at different scan rates to estimate the C _{dl} in a non-faradic potential range.
Figure S12	XPS survey spectrum of anodized SS-75 V electrode after CA test.

Materials characterization

X-ray diffraction (XRD) analysis was performed using a Bruker D2 Phaser operating at 45 kV and 30 mA to examine the crystalline structure of the anodized specimens. Raman spectroscopy measurements were conducted with a Renishaw Raman spectroscope utilizing a 532 nm excitation source. The morphology of the anodized samples was observed under high-vacuum conditions using a Quanta 3D FEG Scanning Electron Microscope (SEM). A platinum layer was deposited using ion beam technology at a 15 kV acceleration voltage to facilitate electron beam observation, achieving a resolution of 1.0 nm, a beam current of 10 pA, and a working distance of 10 mm. Elemental compositions were analyzed through energy-dispersive X-ray (EDX) analysis. The thickness of the oxide layer was determined by analyzing cross-sectional SEM images. Preparation of Transmission Electron Microscopy (TEM) lamella was conducted using a Helios Nano Lab 650 dual beam system, followed by examination using an aberration-corrected Titan 300 ST from FEI at an accelerating voltage of 300 kV. Chemical oxidation state analysis was performed using a Thermo Scientific ESCALAB Xi⁺ X-ray Photoelectron Spectrometer (XPS) Microprobe, employing monochromatized Al (Ka) radiation with a spot size of 650 microns in diameter, operated at 190 W power and 14.5 kV.

Electrochemical Measurements

The electrochemical performance for the Hydrogen Evolution Reaction (HER) and corrosion properties of the anodized stainless steel (SS) electrodes were evaluated using an electrochemical workstation (GAMRY Reference 3000, USA) employing a standard three-electrode configuration at room temperature. The prepared electrodes served directly as working electrodes, while Hg/HgO (1 M KOH) was utilized for HER and saturated Ag/AgCl for corrosion testing as reference electrodes. A graphite rod served as the counter electrode for HER, while a Pt gauze was

employed for corrosion testing. The 1 X 1 cm² working electrode area is soaked in the 1 M KOH electrolyte. Linear sweep voltammetry (LSV) is used at a scan rate of 5 mV s⁻¹ to assess the HER activity of the prepared electrodes. A compensation ratio of 90% is applied to the polarization curve to account for the electrolyte's ohmic resistance. Tafel slopes are calculated by fitting the linear segment of the Tafel curve to the Tafel equation, $\eta = b \log (j) + a$. Electrochemical impedance spectroscopy (EIS) was conducted using an AC voltage amplitude of 5 mV, within a test frequency range of 100 kHz to 1 Hz. Double layer capacitance (C_{dl}) was assessed using the Cyclic Voltammetry (CV) technique within the range of 0.88 to 1.12 (vs RHE) at the different scan rates. Further, the double layer capacitance (C_{dl}) can be converted into electrochemically active surface area (ECSA) by assuming the typical specific capacitance (C_s) value is 0.04 mF cm⁻² for alkaline environments.¹

$$ECSA = \frac{C_{dl}}{C_s} \text{ cm}^2$$

To assess the long-term stability of the prepared electrodes, cyclic voltammetry (CV) tests comprising 2000 cycles were conducted at a scan rate of 100 mV s⁻¹, while chronoamperometry (CA) tests were carried out at a current density of -20 mA cm⁻² for 50 hours. The potentials were converted to a reversible hydrogen electrode (RHE) scale for all HER activity investigations using the following formula.

$$E_{RHE} = E_{Hg/HgO} + 0.0591 \text{ pH} + 0.098$$

To study their corrosion properties, the prepared electrodes were placed in a 3.5% NaCl (neutral environment) solution and a 1 M KOH (alkaline environment) solution. The open-circuit potential (OCP) was first measured for 30 min. Potentiodynamic polarization (PD) experiments were conducted from -0.20 V vs OCP to 0.4 V for NaCl and to 0.3 V vs Ag/AgCl for KOH, using a scan

rate of 10 mV/min. The Tafel module within the Gamry Echem analyst software was employed to compute the Tafel slopes, ascertain the corrosion current density (j_{corr}), and perform extrapolation ± 0.1 V from E_{corr} .

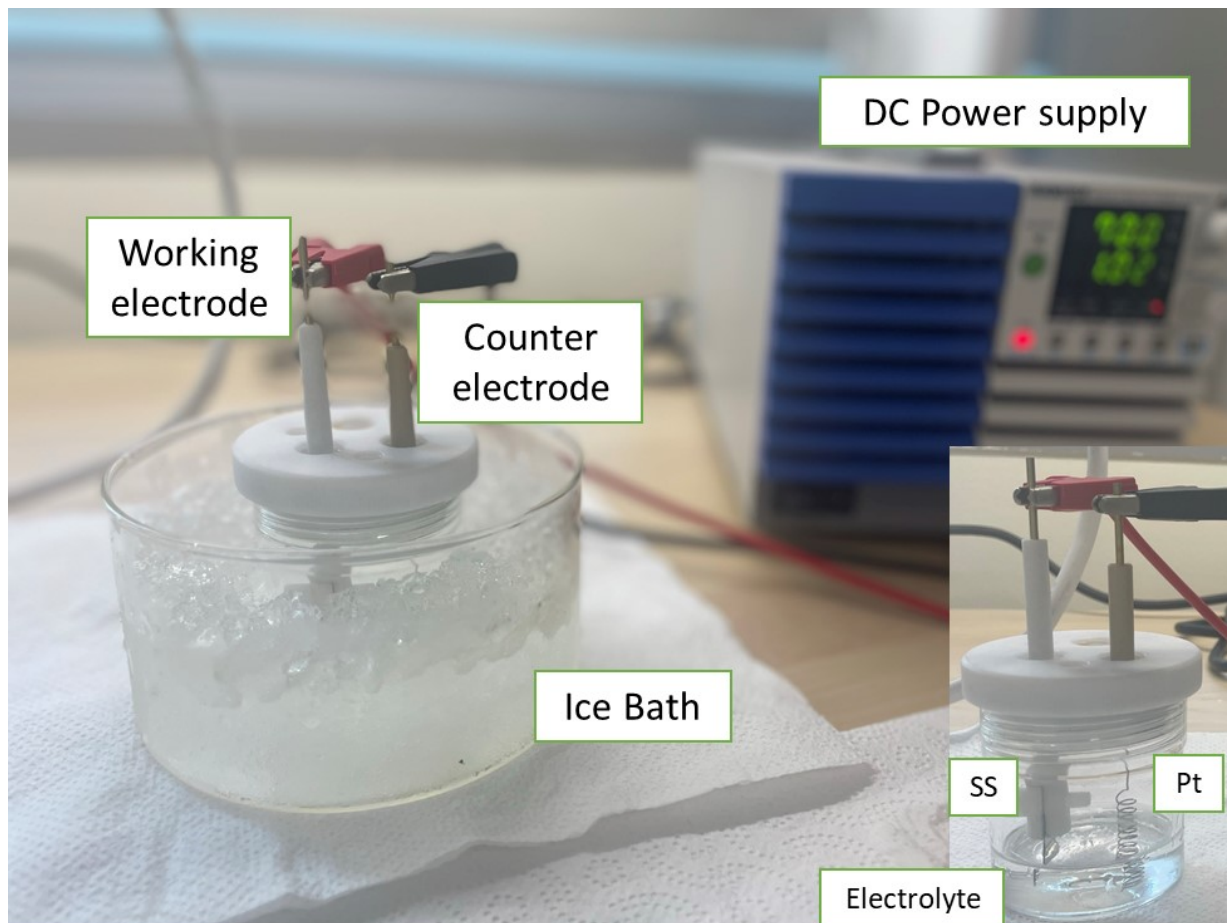


Figure S1. Digital image of an experimental setup for the anodization experiments.

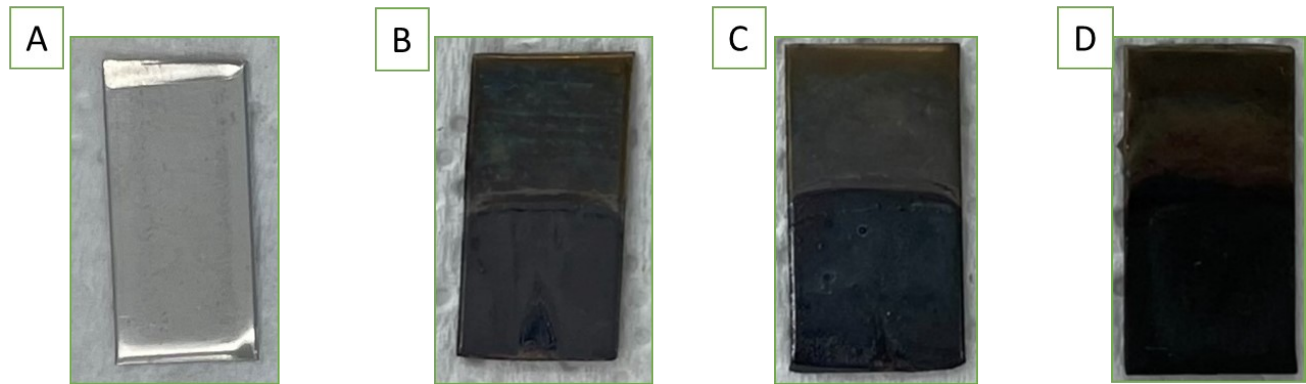


Figure S2. Digital images of bare SS (A), anodized SS samples (B-65 V; C-75 V; D- 85 V)

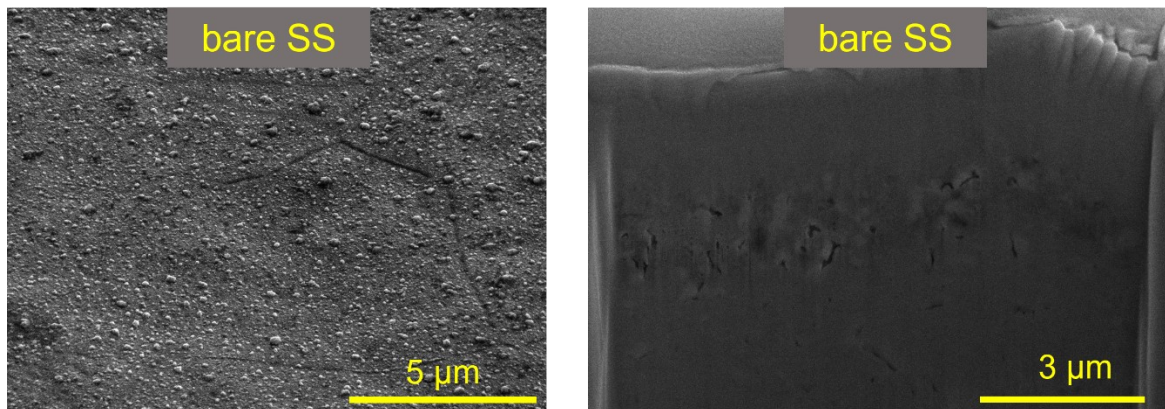


Figure S3. SEM and Cross-sectional images of bare SS²

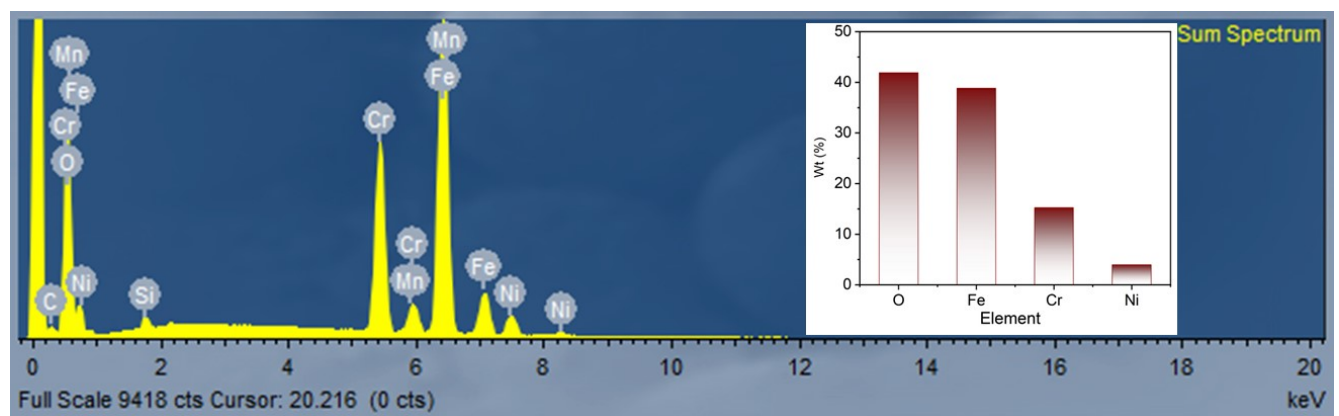


Figure S4. EDX spectrum and weight percentage for major elements of bare SS

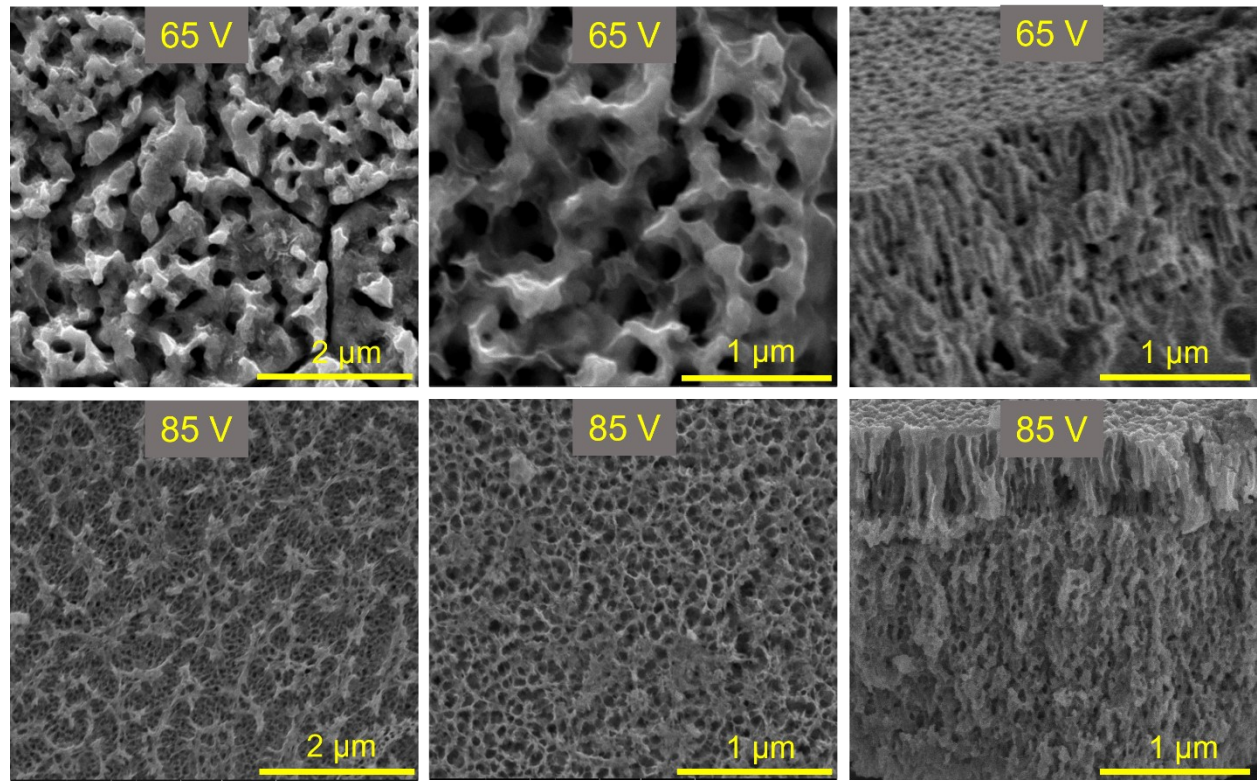


Figure S5. Low and high magnification SEM and Cross-sectional images of anodized SS samples.

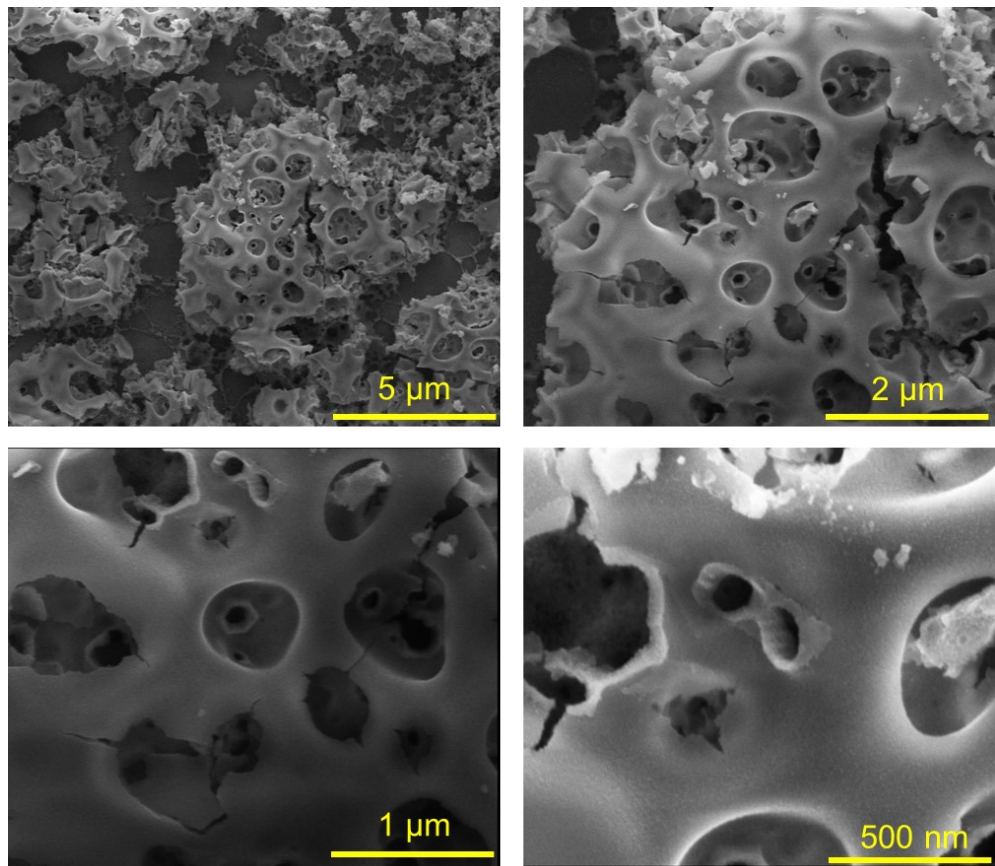


Figure S6. Low and high magnification SEM images of anodized SS-90 V sample

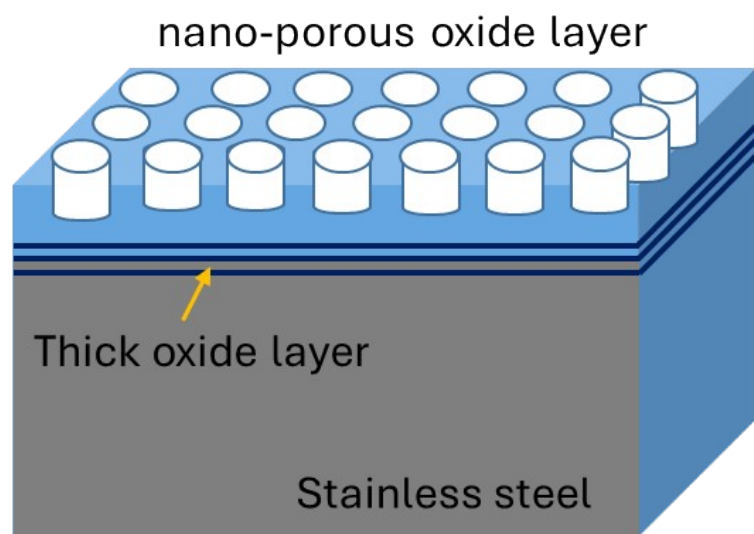


Figure S7. Schematic illustration of anodized stainless steel

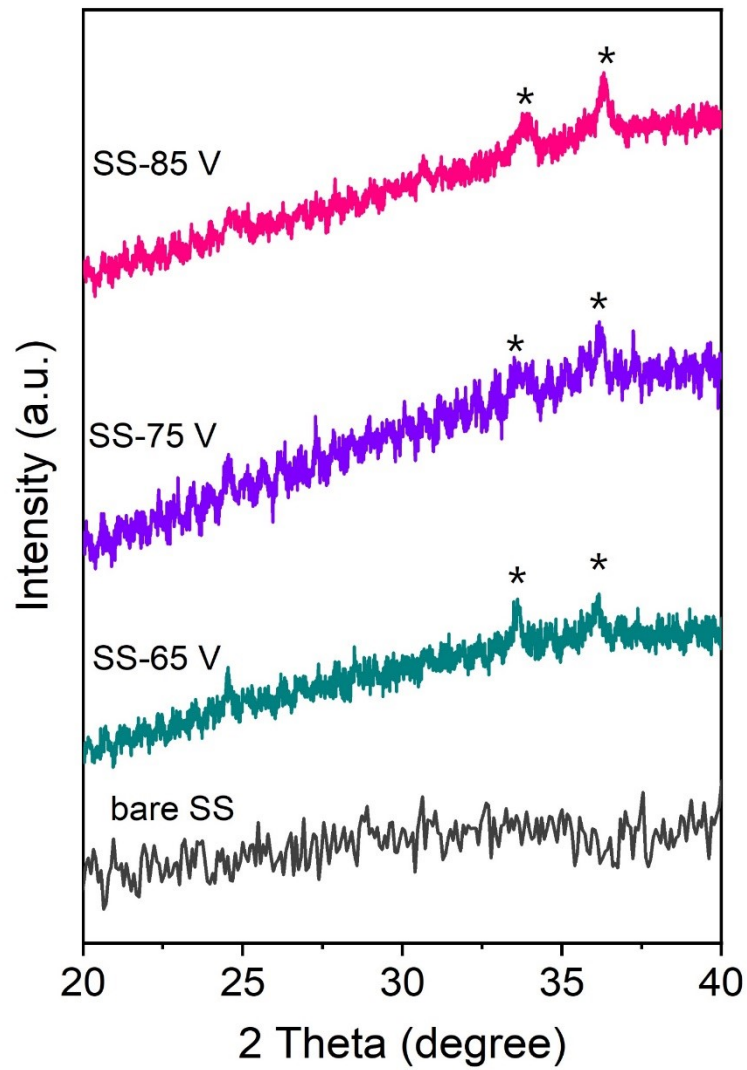


Figure S8. XRD patterns of bare SS and anodized SS samples

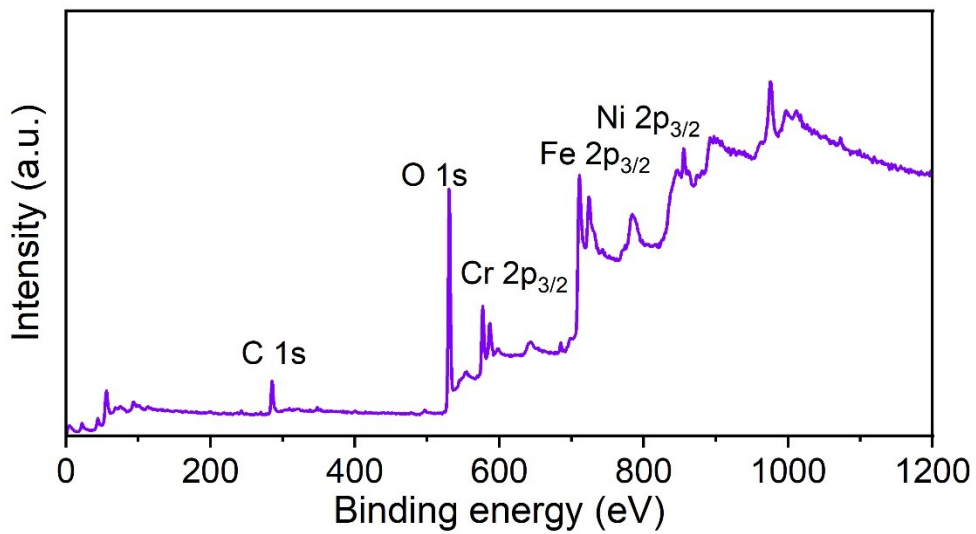


Figure S9. XPS survey spectrum of as-prepared anodized SS-75 V sample.

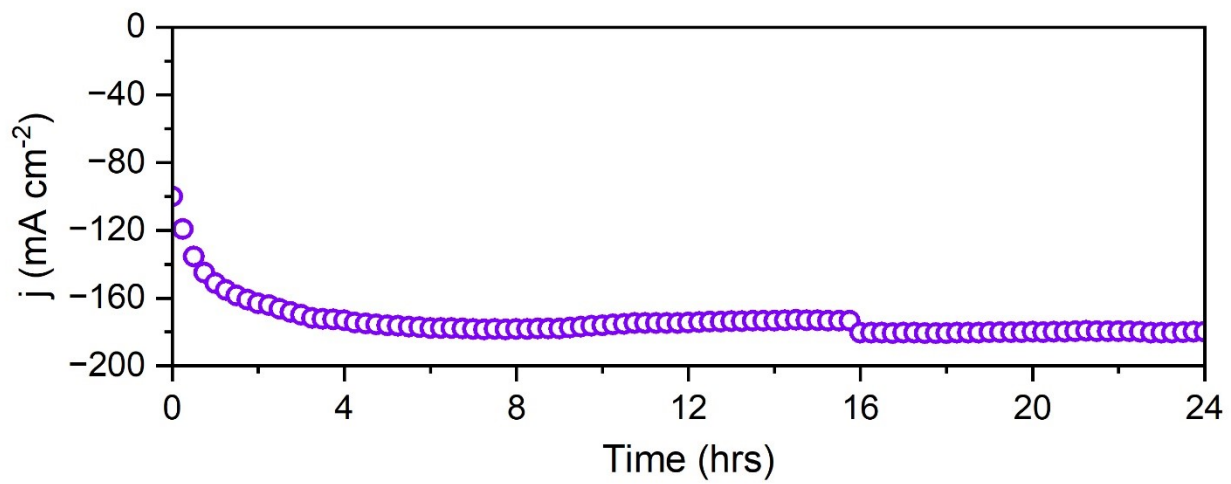


Figure S10. Long-term chronoamperometric (CA) stability measurement at -100 mA cm^{-2} (applied potential -596 mV) for the SS-75 V electrode

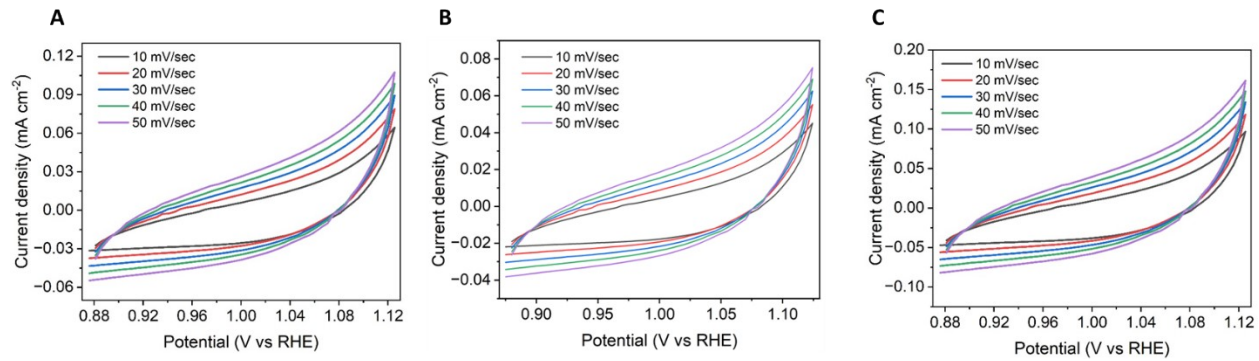


Figure S11. CV curves for anodized SS (A: SS-65 V; B: SS-75 V; C: SS-85 V) at different scan rates to estimate the C_{dl} in a non-faradic potential range.

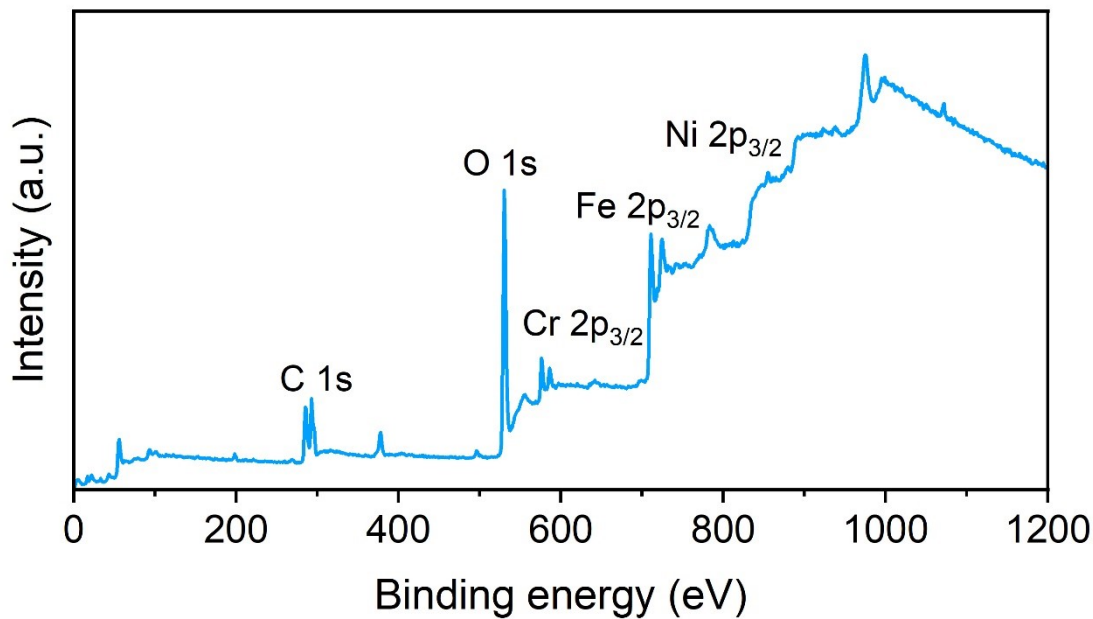


Figure S12. XPS survey spectrum of SS-75 V electrode after long-term (50 h) stability test.

Reference

1. Zhai, L.; She, X.; Zhuang, L.; Li, Y.; Ding, R.; Guo, X.; Zhang, Y.; Zhu, Y.; Xu, K.; Fan, H. J.; Lau, S. P., Modulating Built-In Electric Field via Variable Oxygen Affinity for Robust Hydrogen Evolution Reaction in Neutral Media. *Angewandte Chemie International Edition* **2022**, *61* (14), e202116057.
2. Bose, R.; Suryaprakash Goud, G.; Helal, M. I.; Barsoum, I.; Cho, S. O.; Alfantazi, A., Self-Ordered Anodic Porous Oxide Layers as a High Performance Electrocatalyst for Water Oxidation. *ACS Applied Energy Materials* **2024** (<https://doi.org/10.1021/acsaem.4c00305>).